# DETECTION OF FINE CRACKS BY X-RAY TECHNIQUE USING CONTRAST MEDIUM IN CONCRETE

(Translation from Proceedings of JSCE, No.725/V-58, February 2003)


Koji OTSUKA Mitsuhiro TAKEDA

The purpose of this study is to develop a method for non-destructively detecting the shape and distribution of fine cracks in concrete using X-ray radiography with a contrast medium. First, the conditions under which a dosage penetrates a concrete structure to yield a shadow of moderate density on X-ray film are obtained. Next, experiments on the optimum combination of film, intensifying screen, and crack detectability are carried out. To demonstrate applicability to existing structures, the contrast medium is injected into a reinforced concrete specimen in which a bending crack has been induced, and the location of internal cracks is mapped using this X-ray technique.

***Key Words:*** *X-ray inspection technique, contrast medium, crack identification*

Koji Otsuka is a professor in the Department of Civil & Environmental Engineering at Tohoku Gakuin University, Japan. He obtained his D. Eng. from the University of Tohoku in 1981. His research interests include fracture mechanics of concrete and non-destructive tests of concrete. He is a fellow member of JSCE.

Mitsuhiro Takeda is a professor associate in the Department of Civil & Environmental Engineering at Tohoku Gakuin University, Japan. His research interests include non-destructive tests of concrete. He is a member of JSCE.

## 1. INTRODUCTION

Cases of degradation in which concrete lumps fall away from existing concrete structures are a frequent occurrence. However, it is clear that the life cycle cost of a structure would be lower if repairs were to be carried out prior to such failures — so highly accurate methods of diagnosing concrete structures are required. Non-destructive testing is the primary method of examining degradation and cracking in concrete structures, and the many conventional non-destructive techniques include impact testing, vibration testing, and pullout testing. More recently, methods such as ultrasonic testing, acoustic emission testing, electromagnetic techniques, and X-ray techniques as well as the radar method, electromagnetic induction method, natural electrode potential method, and the infrared method, etc. have come into use. As a result, it is becoming more common to carry out surveys and diagnosis of the internal degradation level of concrete. However, none of the above methods is able to track degradation and damage as it develops. For example, the complicated fine cracking that occurs within a reinforced concrete structure cannot be detected. In fact, no non-destructive method of accurately evaluating the development of small internal cracks has yet been established.

It is clear that the establishment of a technology for the non-destructive detection of internal cracking in concrete structures is an important future goal. To this end, the authors have been pursuing research related to X-ray radiography using a contrast medium [1], [2] for the detection of internal cracking [3], [4] around deformed bars and the tensile fracture progress zone. The present study aims at developing a practical method for non-destructively detecting fine cracks within concrete structures by means of X-ray radiography employing a contrast medium. This equipment and X-ray shielding needed for this method is the same as that employed by the radioparency method — which is used for locating reinforcement and for confirming the condition of mortar filling within sheaths.

Generally, in carrying out non-destructive inspections of concrete structures using X-ray photography, the limit thickness of detectability for a specific material (such as steel plate) is proportional to the rated capacity (tube voltage) of the X-ray source. There are many cases in which output and exposure time are determined by X-ray user in reference to the shown value of the specifications of the X-ray source. However, the X-ray flux varies from device to device even for X-ray sources with the same nominal rating. Further, the image density depends on the developer and type of fixer, as well as their temperature and concentration, while developing and fixing times also differ during X-ray film processing. In addition, when X-ray photographs are taken in the field, it may not be possible to measure the thickness of the target concrete, while on the other hand even if the structure's thickness is known, cracking and peeling degradation may have already occurred externally. This means that the conditions required to obtain images of equivalent density differ according to the context, and it is therefore necessary to determine the relationship between film density and photography conditions by taking test images. Often, though, there is insufficient time for such a field inventory.

There is a clear need to eliminate test photography and simplify the work of testing. The authors consider that such simplification is a prerequisite to the X-ray method coming into more widespread use, and this has led to examination of the basic theory behind X-ray methods. The optimum density of the concrete structure to be examined should be determined in order to produce an X-ray image that can be clearly distinguished by the human eye.

## 2. CONDITIONS FOR CONCRETE X-RAY PHOTOGRAPHY

### (1) Relationship between exposure time and concrete thickness

**Figure 1** illustrates the results of irradiating a concrete specimen using an X-ray source when the X-ray film is in contact with the specimen's rear surface. X-ray energy E that yields the optimum density for the human eye can be approximately expressed with the X-ray source, the irradiated specimen, and the X-ray receptor, when the types of development and fixing liquid, their temperature and concentration, development and fixing times were assumed being constant. Using these factors, the X-ray energy, E, can be written approximately as Equation (1) [5].

$$E = \frac{V^{n} i\, t\, S\, f\, Z}{r^{2} B\, D_a} e^{-\mu_1 d} \qquad (1)$$

Where

E: X-ray energy; V: tube voltage [kV]; n: coefficient related to tube voltage, the presence or otherwise of an intensifying screen, and the absorption of the concrete; i: tube current [mA]; t: exposure time [sec]; S: sensitization ratio of the intensifying screen; f: film sensitivity; Z: atomic number of focus material of X-ray source; r: is the distance from the X-ray source to the specimen [cm]; B: Bucky factor ( the exposure multiple ) when using a grid; Da: area of radiation field [cm$^2$]; $\mu_1$: absorption coefficient of concrete [cm$^{-1}$]; and d: thickness of concrete [cm].

It is possible to replace V , n , i , S , f , Z , r , B , and Da with a single coefficient as long as the photography conditions are constant. Equation (1) can then be written as

$$E = kt\exp(-\mu_1 d) \tag{2a}$$

Where $$k = \frac{V^n\, i\, S\, f\, Z}{r^2\, B\, D_a} \tag{2b}$$

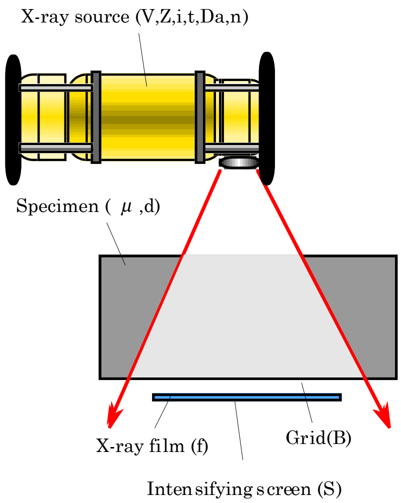


**Fig.1** Photography scheme

Taking the logarithm of both sides of Equation (2a) yields Equation (3a) for exposure time (t ), absorption coefficient ( $\mu_1$), thickness of the structure (d) as follows.

$$\log_e t = \mu_1\, d + k_1 \tag{3a}$$

Where $$k_1 = \log_e E/k \tag{3b}$$

Equation (3a) can be used to generate the exposure chart shown in **Fig. 2**, where the vertical (logarithmic) axis is exposure time t and the horizontal (linear) axis is concrete thickness d, where the straight line has a gradient $_1$ and crossing point $k_1$.

In order to make an exposure chart for use in actual X-ray photography, the optimum film density must first be determined. The film density in the case of incident X-ray flux $I_O$ and transmitted flux $I_t$ can be defined by Equation (4).

$$D = \log_{10}(I_o/I_t) \tag{4}$$

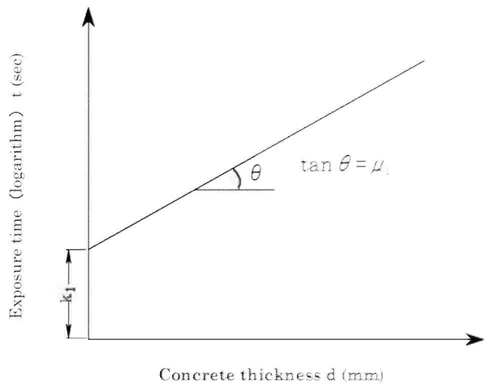


**Fig.2** Relationship between exposure time and concrete thickness

Generally, the range of X-ray film density D is regulated (JIS Z3104) to 1.3-4.0 for areas without defects. The Japanese Society for Non-Destructive Inspection has used radiographic examinations to determine a standard average film density is regulated to 1.0-3.0. Also, transmission photographs exhibit various irregularities caused by reinforcement, aggregate, voids, etc. in the case of a composite material such as concrete. In measuring the density of an X-ray photograph, readings are taken from multiple points with high and low density. To achieve the optimum film density of 2.0 as determined in a preliminary experiment, an experiment aimed at developing an actual exposure chart was carried out. Photography was carried out under the conditions shown in **Table 1**. The concrete mix used for the specimen is shown in **Table 2**.

**Table –1** Photography conditions

| | | |
|---|---|---|
| X-ray source | Tube voltage (V)<br>Tube current (i)<br>Focal distance (r)<br>Focus dimensions | 300kV<br>5mA<br>650mm<br>2.5 2.5mm (tungsten) |
| Concrete | Absorption coefficient ($\mu$) | Average 0.260cm$^{-1}$ |
| Film | Industrial X-ray (f) | Fuji film #50,100,150,400 |
| Grid | Grid density(B)<br>Grid ratio | 40 lines/cm<br>16:1 |
| Intensifying screen | Intensifying screen (S)<br>(Fuji film) | Lead foil screen<br>Fluorescent screen HR-16 |

**Figure 3** shows the exposure chart for film density 2.0 as obtained under the conditions shown in **Table 1**. The vertical axis is exposure time t (sec), and the horizontal axis is concrete thickness d (mm).

**Table –2** Proportions

| Gmax (mm) | (cm) | W/C (%) | Air (%) | s/a (%) | Concrete mix (Kg/m$^3$) | | | |
|---|---|---|---|---|---|---|---|---|
| | | | | | W | C | S | G |
| 20 | 8 | 55 | 2 | 45 | 185 | 336 | 786 | 1025 |

**Figure 3** shows a total of four combinations consisting of X-ray film of #100 or #400 with the metal foil fluorescent screen (HR-16) and X-ray film of #50 or #150 with the lead foil screen. The figure indicates the exposure time needed to obtain a film density of 2.0 in the case of X-rays penetrating concrete up to 200 mm thick.

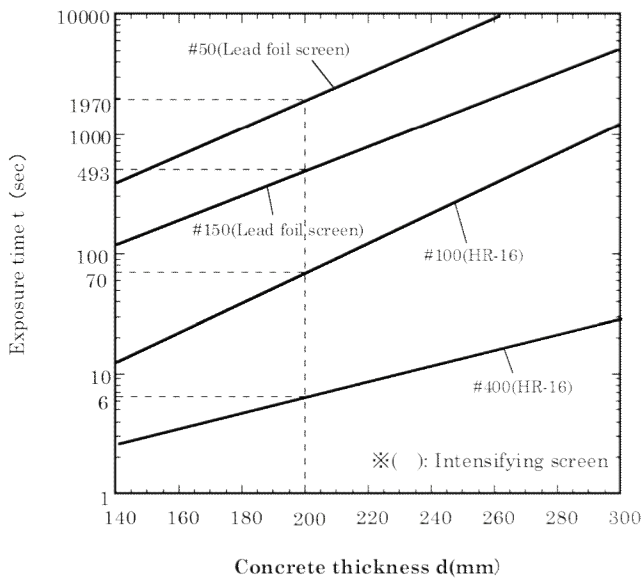


**Fig.3** Exposure chart

Approximately 1,970 seconds of exposure are necessary for #50 X-ray film and the lead foil screen, approximately 493 seconds for #150 X-ray film and the lead foil screen, approximately 70 seconds for #100 X-ray film and the HR-16 intensifying screen, and approximately 6 seconds for #400 X-ray film and the HR-16 intensifying screen.

This demonstrates that the exposure time required to obtain a film density of 2.0 depends greatly on the chosen combination of intensifying screen and film. However, longer exposure times equate to smaller film grain, so the amount of information obtained increases; thus long exposure times are effective for the detection of small details. On the other hand, as the exposure time is reduced, as the film grain becomes bigger, and information is less detailed. It was determined that, in order to detect fine cracks in a concrete structure about 200-300 mm thick, a combination of HR-16 with #100 film (which is relatively fine-grained) is optimum. Still, though the concrete used in this experiment is a typical mix, the optimum combination of film and intensifying screen will depend on the exact characteristics of the concrete.

**(2) Relationship between transmitted X-ray dose and film density**

Degradations such as cracking and peeling generally progress with a structure's use, and X-rays penetrate old structures more easily than sound ones. Therefore, when radioparency photography is used, it is not possible to obtain X-ray images of optimum density through use of an exposure chart derived for sound concrete, such as the one shown in **Fig. 3**. The estimation of photography conditions is further complicated by the presence of steel plates and asphalt.

Generally, photography in the field is preceded by test photography. Following the tests, primary photography takes place. This procedure absorbs time and money. Thus, the relationship between transmitted dose (X-ray dose; unit: $\mu$ Sv) and film density is investigated in this study. Given the availability of the relationship between transmitted dose and film density, it is relatively easy to determine the exposure time required for optimum film density by measuring the transmitted dose in the field using simple equipment such as a pocket dosimeter. Such a method allows fieldwork to be greatly simplified.

Within the range of this experiment, a linear relationship can be assumed between dosage $\beta$ ($\mu$ Sv) and film density D, as given by Equation (5a).

$$D = \alpha \beta \qquad \text{(5a)}$$

Where, $\alpha$ is a coefficient which changes with X-ray film sensitivity, intensifying screen, and the presence or otherwise of a grid.

**Figure 4** shows the relationship between X-ray film density and transmitted dose obtained in the experiment. The X-ray images were taken under the conditions given in **Table 1**. The transmitted dose was measured by installing a pocket dosimeter inside a box (50 x 40 x 150 mm) of 10-mm thick lead in which a 10 mm $\phi$ hole had been formed. The box was fixed on a plane that the hole allows the dosimeter to be irradiated through the hole from the back surface of the specimen, and the transmitted X-ray dose was measured.

The figure demonstrates that the transmitted dose necessary to obtain constant film density is clearly little, because the HR-16 intensifying screen decreases the necessary dose further than the lead foil screen. From **Figure 4(a),** it is clear that the transmitted dose $\beta$ required to achieve density D = 2.0 may be reduced to 23.3 ($\mu$ Sv) by using the #100 X-ray film and the HR-16 intensifying screen. When these values are substituted into Equation (5a), $\alpha$ is found to be 0.086. Consequently, Equation (5a) can be written as Equation (5b).

$$D = 0.086\beta \qquad \text{(5b)}$$

Using the obtained Equation (5b), it is

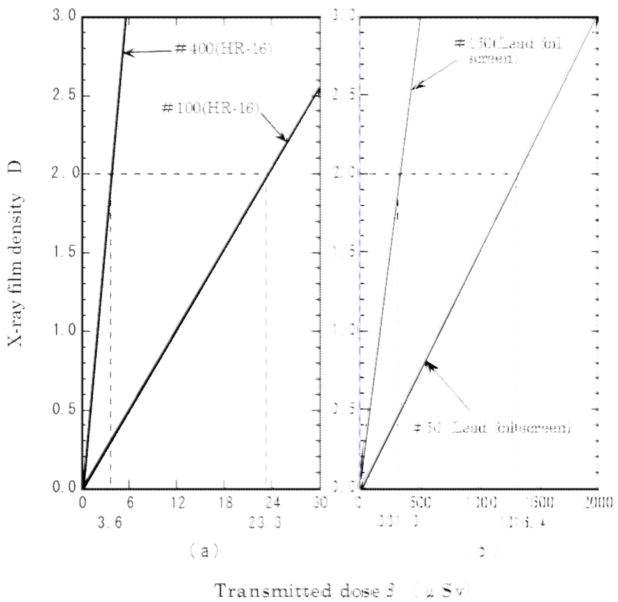


**Fig.4** Relationship between film density and

possible to obtain the resulting film density by substituting the measured value of transmitted dose

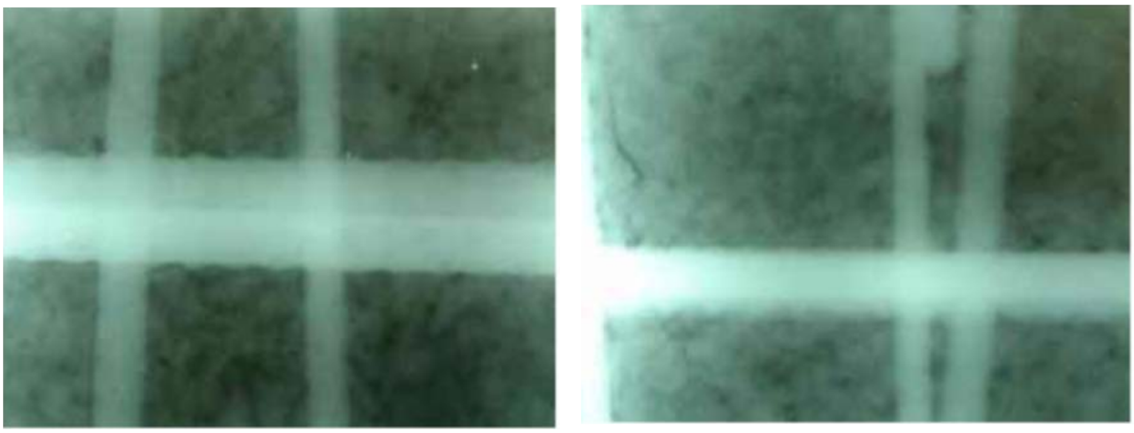

(Sound concrete specimen : Density2.1) (Deteriorated concrete specimen : Density1.9)

**Photograph 1 :** X-ray film image obtained with a constant transmitted doses

of the target structure. Concrete specimens (of dimensions 200 x 400 x 500 mm) were produced in order to verify these results. One sound, reinforced concrete test-piece with no load history and one reinforced concrete specimen in which many cracks had been induced by repeated loading were subjected to a transmitted dose of about 23 ( Sv), and an X-ray image was taken.

**Photograph-1** presents images of the sound specimen (exposure time 36 seconds; transmitted dose 23 Sv) and the deteriorated specimen (exposure time 30 seconds; transmitted dose 24 Sv) taken under conditions given in **Table 1** (#100; HR-16). In comparison with the sound specimen, the exposure time for the deteriorated specimen is shorter. However, these photographs prove that consistent film density can be obtained with a constant transmitted dose. These results lead to the conclusion that, if the transmitted dose is measured in the field, the conditions required for optimum film density can be deduced from the relation between transmitted dose and film density, without the need for test images.

## 3. CONDITIONS FOR PHOTOGRAPHING THE INTERIOR CRACKS USING X-RAY IMAGING

The method described in the previous section allows radioparency photographs of the interior of a deteriorated concrete structure to be obtained at optimum density. Further, radioparency photographs of concrete structures are able to reveal cracks that are comparatively wide. Still, radioparency has difficulty in detecting fine cracks. To overcome this limitation, X-ray radiography with a contrast medium was examined.

The minimum detectable crack width with X-ray radiography and a contrast medium depends on photography conditions, the condition of the subject concrete, the properties of the contrast medium, and other factors, so confirmatory testing for each set of conditions is required. In this study, the conditions adopted are those shown in **Table 1**. The concrete mix was based on that shown in **Table 2**. The contrast medium was a cesium system with an absorption coefficient of 0.43cm$^{-1}$ developed by the authors [6]. Photography conditions for optimum film density were obtained based on the relationship between transmitted dose and film density as described in the previous section. The criterion for determining whether a crack could be observed on the film was the contrast between crack and the surroundings. The X-ray intensity yielding the required contrast is taken to be the exposure radiation dose prior to penetration.

**(1) Relationship between crack thickness and contrast**

When imaging a crack filled with a contrast medium, the ability to detect a crack depends not on the actual crack width, but on the thickness of the crack in the direction of the X-ray axis; that is, the difference in density between crack and the surroundings must be visible on the film.

In **Fig. 5 (a)**, the X-ray power required to penetrated cross section A-A' of the concrete is $I_1$, while the power required to penetrate cross section B-B' (consisting of concrete and a crack containing the contrast medium) is $I_2$. Detection of the crack on film when the X-ray power is Io requires that the contrast in the image produced by $I_1$ and $I_2$ should be visually discernable. On this basis, the X-ray irradiation conditions shown in **Fig. 5 (a)** can be represented by the model in **Fig. 5 (b)**. Here, the crack is filled with the contrast medium and the crack width along cross section B-B' is regarded as the thickness of the contrast medium. In this model, the concrete thickness in cross section A-A' is d and in cross section B-B' it is $d_1$; the thickness of the contrast medium is $d_2$; the absorption coefficient of the concrete is $\mu_1$; and the absorption coefficient of the contrast medium is $\mu_2$. For X-ray power Io as defined above, expressions (6) and (7) can be established.

$$I_1 = I_0\, e^{-\mu_1 d} \tag{6}$$

$$I_2 = I_0\, e^{-(\mu_1 d_1 + \mu_2 d_2)} \tag{7}$$

Equation (8a) is the general expression for X-ray film density D at X-ray power I.

$$D = \gamma \log_{10} I \tag{8a}$$

From this equation, it is clear that if the X-ray film density is $D_1$ with X-ray power $I_1$ and $D_2$ with X-ray power $I_2$, the density difference is D', as follows.

$$D' = D_1 - D_2 = \gamma(\log_{10} I_1 - \log_{10} I_2) \tag{8b}$$

The contrast medium is detectable if D' is greater than the visually distinguishable limit. It is possible here to regard I as a product of tube voltage (keV), tube current (mA), and exposure time (sec). $\gamma$ is a coefficient referred to as film contrast,

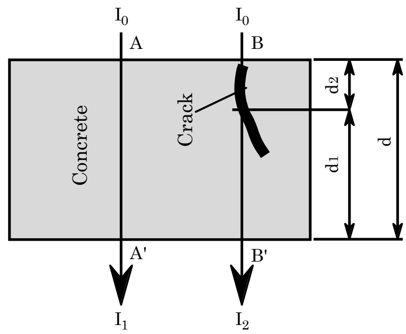

(a) Crack in concrete

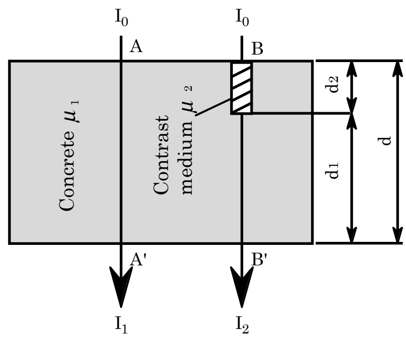

(b) Crack model

**Fig.5** Contrast in X-ray images

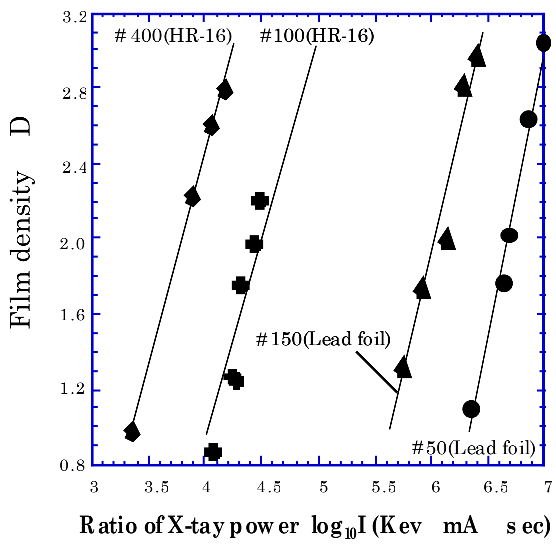

**Fig.6** Relationship between X-ray film density

and its value varies with X-ray power, film sensitivity, and the existence of an intensifying screen. Therefore, it is necessary to acquire $\gamma$ by experiment in each and every case.

**Figure 6** shows the relationship between film density and $\log_{10}I$ as acquired by experiment. Photography was again carried out under the conditions given in **Table 1**. The gradient ($\Delta D'/\Delta \log_{10}I$) near a film density of 2.0 when using a #100 X-ray film and an HR-16 intensifying screen was 2.04. This yields the film contrast coefficient $\gamma$ as given by Equation (9).

$$\gamma = \frac{\Delta D'}{\Delta \log_{10} I} = 2.04 \tag{9}$$

Next, the test equipment illustrated in **Fig. 7** was used to determine the minimum detectable contrast medium thickness; only concrete thickness and contrast medium thickness were varied in the experiment. The images were made with #100 film and an HR-16 intensifying screen. The concrete specimen was varied from about 140 mm to about 300 mm in thickness, and a special board on the irradiation plane was mounted with chloroethylene pipes of various diameters ($\phi$0.3, 0.6, 0.8, 1.0, 1.5, 2.0, and 3.0 mm) filled with the contrast medium to represent cracks. This yielded the smallest detectable crack width for each specific concrete thickness, and it was the lowest contrast which could distinguish this time contrast in the present experiment.

**Photograph 2** gives X-ray images obtained in this experiment. The upper photograph was taken with a concrete thickness of 143 mm, while the lower one was with a concrete thickness of 225 mm. These images show that all pipes can be detected when the thickness of the concrete specimen is 143 mm. However, contrast medium with a thickness of over 0.6 mm is detectable when the concrete thickness is 225 mm, while 0.3 mm and thinner pipes filled with contrast medium are undetectable.

**Figure 8** shows the relationship between concrete specimen thickness and required contrast medium thickness based on the results of this experiment. The curve in the figure represents the detectable limit. It is clear that the minimum detectable contrast medium thickness increases with concrete thickness.

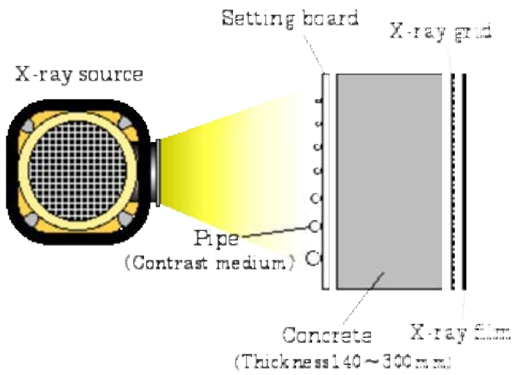


**Fig.7** Experimental method

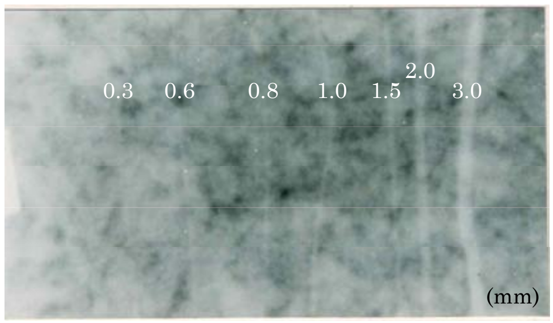


Concrete thickness 143mm,Film sensitivity #100

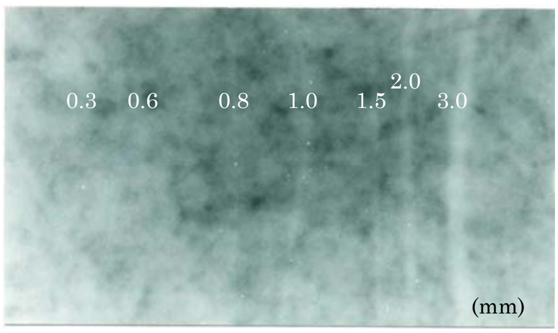


Concrete thickness 225mm, Film sensitivity #100

**Photograph 2** X-ray images with contrast medium filling pipe

When the pipe containing contrast medium is placed on the concrete surface as shown in **Figure 7**, X-ray power $I_2$ that penetrates the crack is determined by Equation (10), because $d_1$ in **Figure 5** becomes d.

$$I_2 = I_0\, e^{-(\mu_1 d + \mu_2 d_2)} \qquad (10)$$

That is, contrast C is required for detectability at each concrete thickness. Equation (8b) has already proven that density difference D' requires contrast C. Therefore, Equation (8b) can be rewritten as Equation (11) by substituting Equations (6) and (10) into Equation (8b).

$$C = \gamma\, \mu_2\, d_2 \log_{10} e \qquad (11)$$

This formula establishes the visible contrast with which the contrast medium appears on X-ray film. By substituting the minimum detectable contrast medium thickness into this equation, the values of C listed below are obtained.

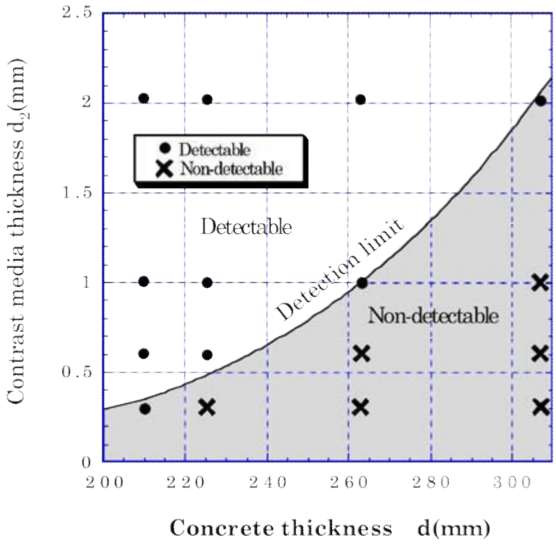


**Fig.8** Relationship between detectable crack thickness and concrete thickness

For concrete thickness 143 mm and 210 mm : C≒0.01 ( $\gamma$=2.04; $\mu_2$=0.43/cm; $d_2$=0.03 cm)
For concrete thickness 225 mm : C≒0.02 ($\gamma$=2.04; $\mu_2$=0.43/cm; $d_2$=0.06 cm)
For concrete thickness 263 mm : C≒0.04 ($\gamma$=2.04; $\mu_2$=0.43/cm; $d_2$=0.10 cm)
For concrete thickness 307 mm : C≒0.08 ($\gamma$=2.04; $\mu_2$=0.43/cm; $d_2$=0.20 cm)

The minimum contrast generally distinguishable by the human eye is regarded here as 0.01 [5]. In this experiment, contrast C≒0.01 is obtained; consequently Equation (11) seems applicable for specimens of thickness 210 mm or less. However, the detectable contrast C calculated by Equation (11) exceeds 0.01, when the concrete thickness is over 225 mm. This is probably due to the effect of X-ray scatter, leading to over-estimation.

Generally, X-rays are attenuated by absorption and scattering during passage through concrete. Coefficient $\mu_2$ in Equation (11) represents the sum of photoelectric effect coefficient $\tau$ (absorption) and the Compton coefficient $\sigma$ (scattering). The Compton effect becomes dominant when the X-ray source voltage is high (300 kV), as in this experiment; on the other hand, the photoelectric effect is dominant when the X-ray output is low. With increased concrete thickness, Compton scattering will increase as the exposure time is extended. In this respect, though the scattering of X-rays is taken into account in Equation (11), further examination is needed regarding the effect of scatter beyond a concrete thickness of 225 mm. This is a subject for future research.

**(2) Relationship between crack position in the concrete and contrast**

In the experiment described above, cracks were represented by pipes containing the contrast medium on the surface of the concrete specimen. Next, pipes containing the contrast medium were embedded at various depths below the concrete surface, and similar X-ray photography carried out. The test equipment is shown in **Fig. 9**. The concrete specimen contains pipes of 0.3 mm diameter filled the contrast medium spaced at 10 mm intervals of depth from the irradiation plane. Specimens of increasing thickness were used until detection of the pipes filled with contrast medium became difficult. Photography was carried out using #100 X-ray film and an HR-16 intensifying screen under the conditions given in **Table 1**.

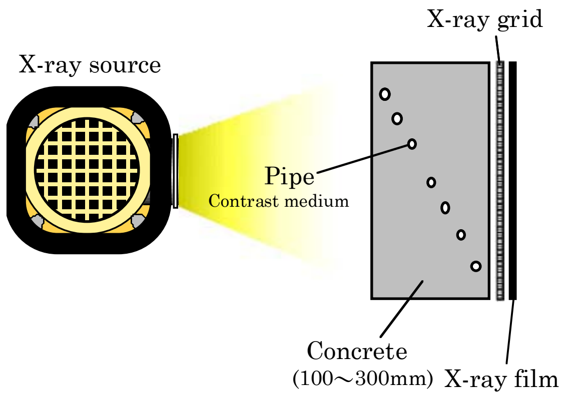


**Fig.9 :** Test equipment

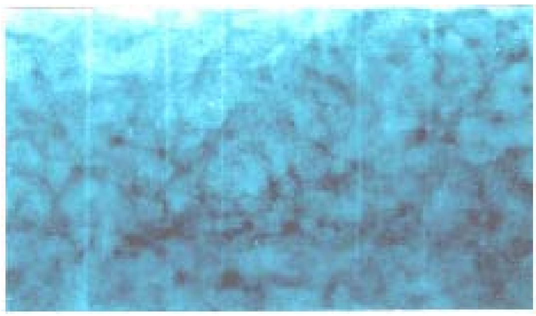

**Photograph 3 :** X-ray image with contrast medium filling pipe

**Photograph 3** shows the resulting X-ray image for the 180-mm thick specimen. The numerals in the figure give the distance (mm) of the pipe from the irradiation plane. This image has a contrast exceeding 0.01 for simulated cracks within the concrete, and detectability is little different from the previous experiment. However, the contrast became zero for concrete thicknesses of 225 mm and above; at this point, detection of the pipes at all depths became impossible. Pipes of 1.0 mm were substituted in specimens of thickness greater than 265 mm, and photography carried out in a similar experiment. Detection was found to be impossible, since the contrast was zero in all cases. This demonstrates that the diameter of the pipe in a particular specimen is irrelevant to detectability with regard to the depth direction, and X-ray film contrast was almost the same regardless of pipe diameter.

## 4. CRACK DETECTION IN CONCRETE SPECIMENS

In order to confirm whether the results obtained above can be applied to an actual concrete structure, the contrast medium was injected into bending cracks induced in reinforced concrete specimens, and X-ray photography was carried out.

### (1) Experimental method

**Figure 10** shows the specimens used for the experiment. The geometries of the specimens were 200 x 200 x 550 mm and 200 x 250 x 550 mm, respectively, with 5 specimens of each size for a total of 10 specimens. Each contained one deformed D13 bar. A non-penetrating bending crack was induced in each specimen by 3-point loading. The resulting crack width was 0.2 mm at the surface of the specimen of thickness 200 mm, and 0.7 mm at the surface of the specimen of thickness 250 mm.

The pipe used to inject contrast medium was put in place after cracking, and the crack plane was

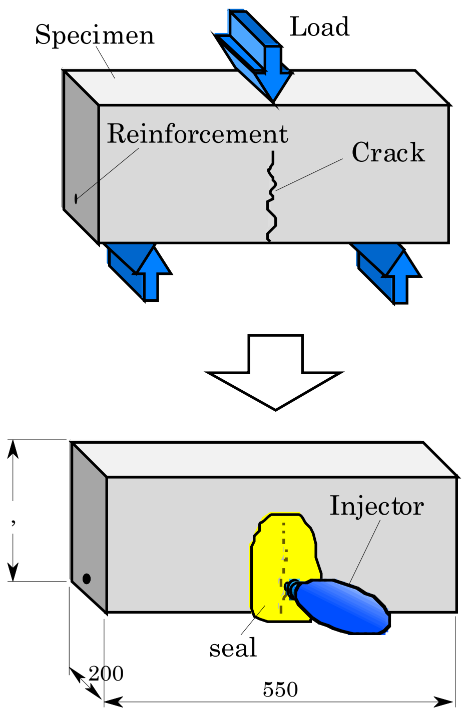


**Fig.10 :** Specimen manufacture method

sealed around the pipe. After allowing the seal coating to harden, the specimen was photographed prior to introducing the contrast medium. The contrast medium was then injected at a pressure of 0.3 N/mm2, and the specimen was irradiated with X-rays in the basal plane direction (the crack opening side) to obtain an X-ray image.

The transmitted dose was measured using a pocket dosimeter in order to determine the exposure time. Photography conditions were based on those given in **Table 1**. The optimum transmitted dose for X-ray film #100 and an HR-16 intensifying screen was derived from **Fig. 4**, and then adjusted to 23 ($\mu$Sv). Then, for the specimens of 200 mm and 250 mm thickness, respectively, the exposure time was 70 seconds and 289 seconds.

**(2) Experimental results**

**Photograph 4** shows the results for the specimen of thickness 200 mm, with image (a) obtained before injection of the contrast medium and image (b) obtained with the contrast medium in the crack. The maximum density in both images is close to 2.0. In these photographs, the thick horizontal line on the X-ray film is the deformed bar, while the thin vertical line is the gage mark rod made of lead. The vertical black shadowy area in image (a) and the vertical, meandering white bundle in image (b) are the detected cracks. Though in image (a) taken before injection of the contrast medium, there is some evidence of the black crack, it is not clear. However, it is possible to see a clear crack group in the image taken after injection.

The results for the specimen of 250 mm thickness showed similar results; clear cracking was visible after injection of the contrast medium, though an indistinct black crack was visible without the medium. In this case, however, crack visibility was lower than in the thinner specimen.

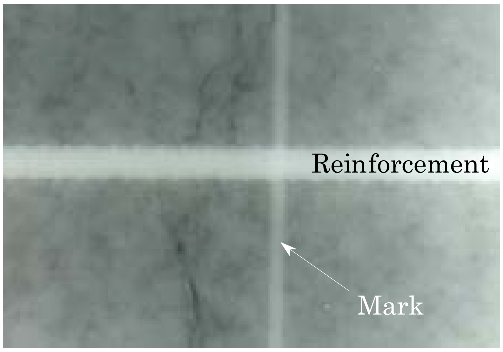


(a)Before contrast media injection

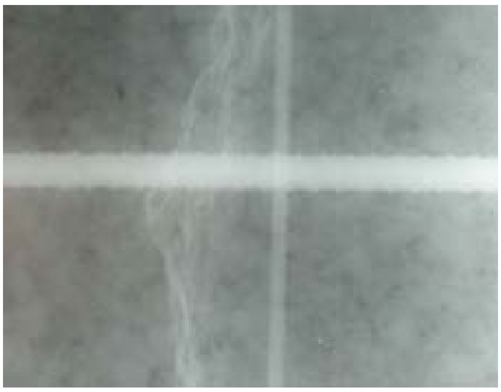

(b)After contrast media injection

**Photograph 4** X-ray film (thickness 200mm)

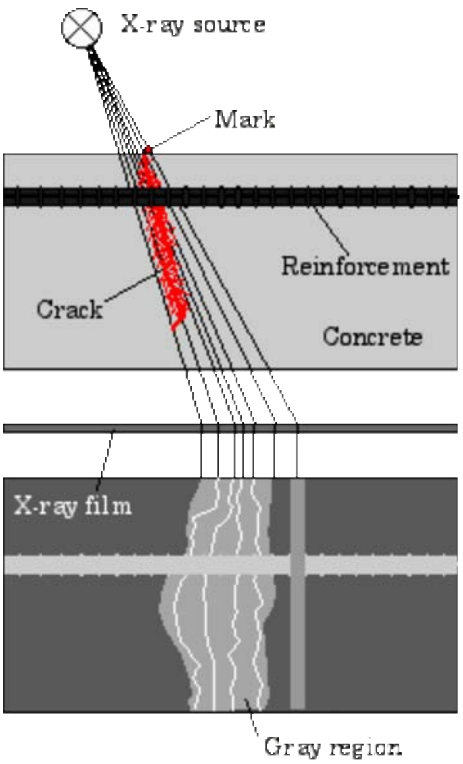


**Fig.11** Image projected by X-ray film

These experimental results indicate that cracks are detected on film as groups of clear, white, wavy lines and dim gray region when a contrast medium is used. The gray region seems to be where the contrast medium has permeated very fine cracks branching out from the main crack, and where the crack is not aligned with the irradiation axis.

**Figure 11** illustrates this. It can be said that the crack will be detected if the part of the crack parallel or nearly parallel to the irradiation axis is longer than the detectable contrast medium thickness indicated in **Fig. 8**.

## 5. MEASUREMENT OF CRACK TIP POSITION

When a non-penetrating crack occurs in a concrete structure, it is important to examine the depth of the crack when assessing its influence on structural strength. The use of X-ray radiography with a contrast medium makes it possible to determine the crack tip position. Here, as a supporting experiment, a non-penetrating crack was induced in a reinforced concrete specimen, and the crack tip position was measured [7]-[10].

### (1) Experimental method

The tip of a non-penetrating crack in a concrete structure can be located by moving the X-ray radiography source to two different locations near the mouth of the crack. **Figure 12** shows this measurement method. The parallax of the crack tip between the two images is n, the parallax of the gage mark is m, the distance from the X-ray source to the irradiation surface is $L_1$, and the X-ray source is moved by distance M. Thickness of the structure t is given by Equation (12).

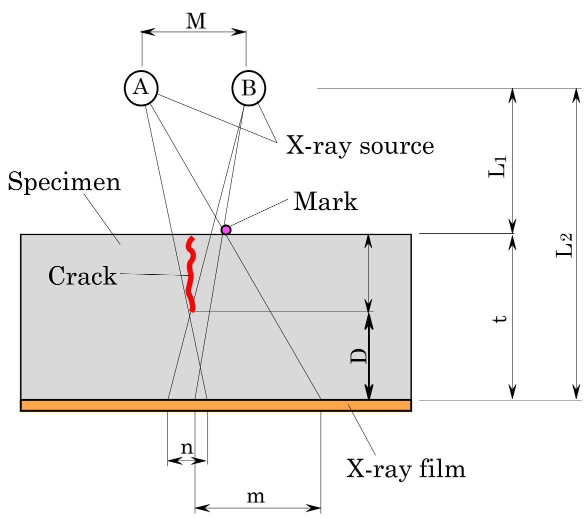


**Fig.12** Crack tip position measurement method

$$t = m\frac{L_1}{M} \qquad 12$$

The un-penetrated length D is then:

$$D = \frac{n\ (L_1 + t)}{M + n} \qquad 13$$

Therefore, it is possible to obtain length $\ell$ from the surface to the crack tip using Equation (14).

$$\ell = t - D \qquad 14$$

For the experiment, five specimens (180 x 250 x 500 mm) of the shape as shown in **Fig. 11** were used. After injecting the contrast medium into the bending crack (which measured about 0.2-0.5 mm in opening width), multiple images were obtained with the X-ray source in different positions. The crack tip position was then calculated.

### (2) Experimental results

**Photograph 5** shows the X-ray images obtained for source locations A and B after the contrast medium was injected into the crack. Based on these images, crack tip positions were determined using Equations (12), (13), and (14); examples are plotted in **Fig. 13**. This figure shows the crack

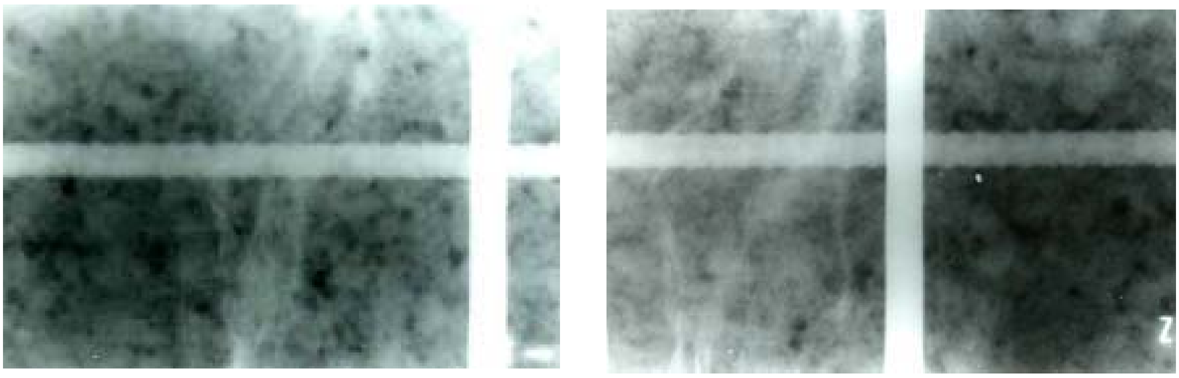

(a) Photographing from A point (b) Photographing from B point

**Photograph 5** X-ray image

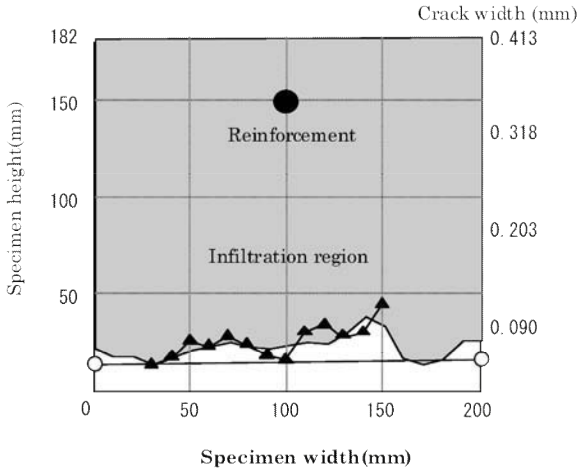


**Fig.13** Crack tip position

cross section. The vertical axis represents specimen height, a, and the horizontal axis is specimen width. The "○" marks in the figure represent the tip of the crack as confirmed by visual observation of both sides of the specimen for the case of a non-penetrating crack (crack width of 0.413 mm) induced in the specimen by 3-point bending. The shaded region of the figure represents the area permeated by the contrast medium; after the experiment, this was examined by destroying the specimen. The coloring by red ink was carried out in order to highlight the region into which the contrast medium was injected. The "▲" marks in the figure represent the crack tip position based on the X-ray images.
From this figure, the error between the actual crack positionand the crack tip position calculated from the X-ray images is about 5 mm, so there is considerable agreement. The width of the crack tip was found to be about 0.02-0.09 mm and the tip area was filled with contrast medium, which made crack detection possible.

## 6. DETECION OF CRACK SHAPE

If the internal shape of a crack induced in a concrete structure could be examined, it would be possible to make deductions regarding the direction of the force causing the crack and whether the crack has continued to grow. It would also be possible to predict the future direction in which the crack will develop, and this could provide important data regarding durability estimates and the need for reinforcement of the structure. Based on the position of the crack tip and by using X-ray radiography with the contrast medium, it should be possible to reveal the internal shape of the crack. A basic experiment was carried out to detect the internal shape of cracks induced in specimens (100-150 mm in thickness) [11].

## (1) Experimental method

### a) Crack shape measurement method

**Figure 14** shows the principle of crack shape detection. X-ray radiography is performed using the contrast medium at two points (A and B in the figure). The position of point A is perpendicular to the front mark. The calculation method is similar to that used for the measurement of the crack tip position. The X-ray source is moved from point A to point B, and from the parallax of the gage mark on the X-ray image and the parallax of the crack parallel or nearly parallel to the irradiation axis, it is possible to obtain the vertical depth ($\ell$) of each crack turning point using Equations (12)-(14). It is then possible to acquire the horizontal distance (H) from the rear mark to the crack turning point using Equation (15).

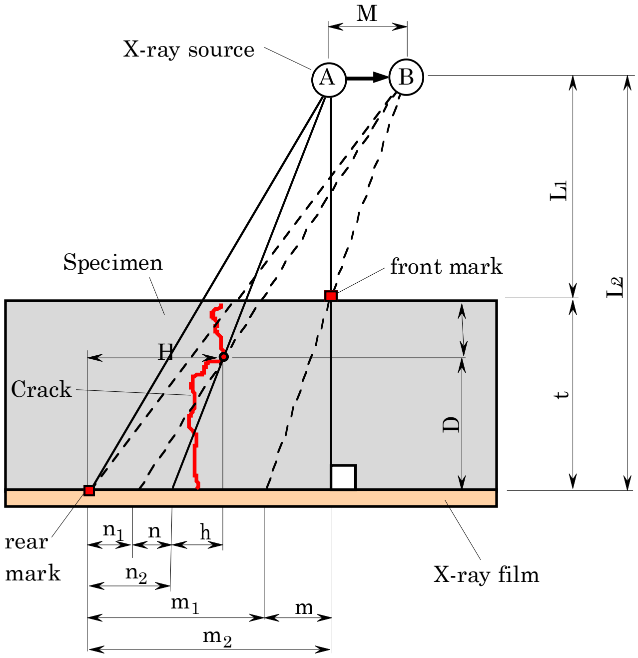


**Fig.14** Crack shape detection method

$$H = n_2 + \frac{n(m_2 - n_2)}{M + n} \qquad 15$$

### b) Experimental specimens and photography method

In the experiment, rectangular concrete columns measuring 100 x 100 x 400 mm and 100 x 150 x 400 mm were used as specimens. The concrete mix was as shown in **Table 2**. The specimens were fractured by 3-point bending test. Therefore, after the shape of the fracture surface of specimen was measured, it was refitted to the fracture surface, and other all planes except for the upper surface were coated with sealing compound. Next, the gage mark necessary for measurement from the X-ray images was bonded to the specimen surface. Images were obtained under the conditions given in **Table 1** using #50 X-ray film and a lead foil screen.

## (2) Experimental results

**Photograph 6** shows examples of a crack image from site A and one from site B 46 mm distant. Using these two X-ray images, it was possible to observe the crack three-dimensionally using stereoscopy and a mirror-style stereoscope. As the result, it was

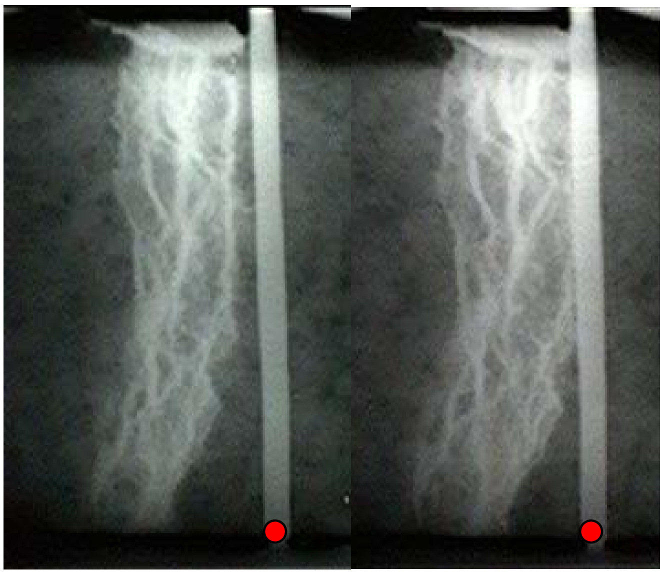

Left photograph Right photograph

**Photograph 6** X-ray image

confirmed that the turning point of the ruggedness of a crack surface could be projected in multiple wave lines onto film. The position of the turning point was then calculated based on the parallax of the crack as revealed by the two X-ray images.

**Figure 15** compares the crack shape calculated from the X-ray images with the actual shape observed on the fracture surface. The triangular mark calculated from X-ray film in the figure shows the shape of the crack surface at positions 20mm and 40mm from the upper surface of the specimen. These results demonstrate that the crack shape as determined from the X-ray images closely matches the actual crack shape.

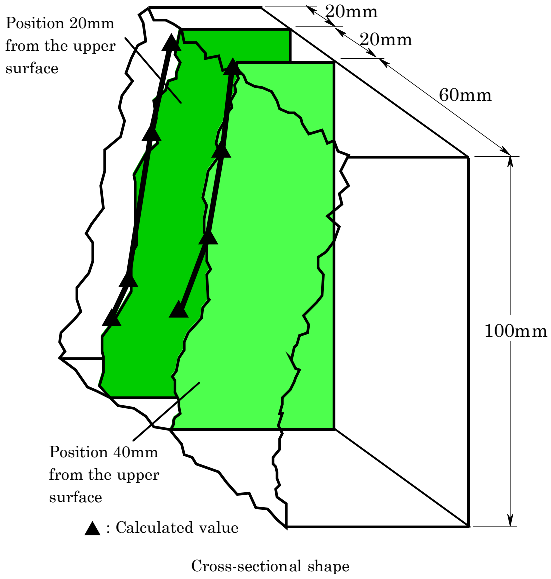


**Fig.15** Crack shape measurement result

## 7. CONCLUSION

The purpose of this study was to develop a technique for the non-destructive detection of cracks within concrete structures using X-ray radiography and a contrast medium. The following conclusions can be drawn from the experiments carried out:

(1) The X-ray energy needed to produce optimum density on the X-ray film was theoretically examined. The relation between concrete thickness and X-ray irradiation time for various combinations of films and intensifying screens was established in the form of an exposure chart. Such a chart had not been previously available.

(2) The combination of #100 film, whose particles are comparatively small, an HR-16 screen, and a relatively short exposure time proved optimum for detecting cracks within the concrete.

(3) It was shown possible to obtain the optimum film density based on the relation with transmitted dose without the need for test photography, assuming that the transmitted dose can be measured in the field.

(4) By placing contrast medium-filled pipes with an inside diameter of 0.3-2.0 mm on the irradiation surface of a concrete specimen to simulate cracks, it was possible to determine the relationship between contrast medium thickness (pipe inside diameter) and concrete thickness from the resulting X-ray images. It was also demonstrated that detectability was diminished by the effects of X-ray scattering as the thickness of the concrete increased.

(5) Contrast medium-filled pipes (of diameter 0.3 mm) were set at various depths within concrete specimens, and using X-ray photography it was proven that there was no relation between contrast medium detection accuracy and depth.

(6) When the contrast medium was injected into an actual crack, clear white wavy lines and gray regions were seen in the resulting X-ray images. It is concluded that the clear white lines represent an area of multiple fracturing where the main crack is along the X-ray axis. The gray region seems to be where the contrast medium has permeated fine cracks that branch out from the main crack, many at nearly a right-angle to the X-ray axis.

(7) The position of a non-penetrating crack in a concrete structure was demonstrated by measuring

the location of the crack tip from the mouth using a technique in which images were taken with the X-ray in two different slightly separated locations. Using a specimen with a thickness of 180 mm it was possible to determine that the error between the calculated tip position and the contrast medium penetration depth was small.

(8) It was possible to determine the internal shape of a crack by X-ray radiography with the contrast medium; this was done by obtaining one image with the X-ray source perpendicularly above a gage mark and another from a nearby position, and analyzing the two resulting images. By cracking open and examining the specimens (100 mm in thickness and 150 mm in thickness), it was proven that the actual crack shape and the crack shape depicted by the X-ray images closely agreed.

**References**


[1] Otsuka, K.: X-Ray Technique with Contrast Medium to Detect Fine Cracks in Reinforced Concrete, International Workshop on Fracture Toughness and Fracture Energy (Sendai, Tohoku Uni.), 1988.10

[2] Otsuka, K.: Detection of Fracture Process Zone in Concrete by Means of X-Ray with Contrast Medium, Fracture Mechanics of Concrete Structures, Elsevier Applied Science, pp.485-490, 1992.6

[3]Otsuka, K: Detection of fine cracks in reinforced concrete by X-ray techniques using contrast medium, Proceedings of the Japan Concrete Institute, Vol.10, No.3, pp.145-150, 1988.10

[4] Otsuka, K: Detection of fine cracks in reinforced concrete through X-ray techniques using contrast medium, Journal of materials, concrete structure and pavements, No.451/V-17, pp.169-178, 1992.8

[5] Uchida, M., Yamashita, K., and Inatsu, H.: Image engineering for the radiation engineer, tsuushou-sangyou-kenkyusha, 1978.7

[6] Patent No. 2113200: X-ray contrast medium and crack detection method for concrete, 1996.11

[7] Mitsuhiro, T., Otsuka, K., and, Sano, T: The development of crack inspection technique for concrete structures by X-ray radiography with contrast medium, Proceedings of the 50th JSCE Annual Meeting, pp.664-665, Ehime, 1995.9

[8] Mitsuhiro, T., Otsuka, K., and, Sano, T.: Research on tip position measurement of non-penetrating crack in concrete structure, Proceedings of the 51st JSCE Annual Meeting, Vol.V, pp.1168-1169, 1996.9

[9] Otsuka, K., and Takeda, M.: Detection and Simultaneous Repairing of Cracks in Reinforced Concrete Structures, 1997 International Conference on Engineering Materials, Volume , pp89-98, 1997.6

[10] Otsuka, K., and Takeda, M.: Injection Material for Cracks Combining Function of Repair and X-Ray Contrast, 25th Anniversary Conference on Our World in Concrete & Structures, Singapore, pp.507-514, 2000.8

[11] Otsuka, K., and Takeda, M.: Research on internal shape detection of cracks in concrete structures, Proceedings of the 52nd JSCE Annual Meeting, Vol.V, pp.692-693, 1997.